THE ASTROPHYSICAL JOURNAL, 476:620–631, 1997 February 20

X-RAY VARIABILITY AND CORRELATIONS IN THE TWO-PHASE DISK-CORONA MODEL FOR SEYFERT GALAXIES

FRANCESCO HAARDT[1,2]
Department of Astronomy and Astrophysics, Institute of Theoretical Physics, Göteborg University and Chalmers University of Technology, 412 96 Göteborg, Sweden

AND

LAURA MARASCHI AND GABRIELE GHISELLINI[1]
Osservatorio Astronomico di Brera/Merate, 20100 Milano, Italy
Received 1996 June 18; accepted 1996 September 16

ABSTRACT

We discuss in detail the broadband X-ray variability expected in Seyfert galaxies in the framework of a Compton-cooled corona model, computing spectral indices in the 2–10 keV range and fluxes in the medium (2–10 keV), hard (30–100 keV), and soft (0.1–0.4, 0.9–2 keV) X-ray bands, for different hypotheses concerning variability "modes." In all cases the soft photons responsible for the cooling are assumed to be proportional to the Comptonized flux (fixed geometry), and the plane-parallel limit is adopted. Variations in the optical depth τ of the corona cause spectral changes in the Comptonized emission in the sense that the spectrum steepens and the temperature decreases with increasing τ. If the corona is pair dominated, τ is determined by the compactness (proportional to luminosity for fixed size). This yields a definite relation between spectral shape and intensity, implying a variation in intensity of a factor 10 for a change of 0.2 in the 2–10 keV spectral index. For low pair density coronae, no definite prediction is possible. If, for instance, τ varies while the luminosity remains approximately constant, the Compton spectrum shows a pivoting behavior around $\simeq 10$ keV. In both cases, the coronal temperature decreases for increasing spectral index. In the absence of substantial changes in the structure of the corona, the soft thermal component correlates with the medium and hard Comptonized components. Although the correlation must hold globally, that is, for the integrated power of the two components, the observed intensity in the soft X-ray band is extremely sensitive to the temperature of the thermal component that may vary as a result of variations in luminosity and/or area of the reprocessing region(s). Examples are computed using the *ROSAT* response matrix, showing that for $kT \lesssim 60$ eV the spectrum in the *ROSAT* range softens with increasing intensity while the opposite is true for larger temperatures. Current observations of NGC 5548 and Mrk 766 showing different behaviors can therefore be reconciled with the model. The spectral behavior of Mrk 766 strongly suggests that the coronal plasma in this source is not pair dominated. The possibility of constraining models through simultaneous observations in the soft, medium, and hard X-ray ranges is discussed.

Subject headings: accretion, accretion disks — galaxies: Seyfert — X-rays: galaxies

1. INTRODUCTION

The observations of OSSE on the *Compton Gamma Ray Observatory* showing a break or an exponential cutoff in the high-energy spectrum of some Seyfert galaxies (Maisack et al. 1993; Johnson et al. 1993; Madejski et al. 1995) coupled with the X-ray observations of *GINGA* have had a strong impact on our theoretical understanding of the X-ray and γ-ray emission processes in these objects. Although they do not rule out pure nonthermal $e^{\pm}$ pair models (Zdziarski, Lightman, & Maciolek-Niedzwiecki 1993), thermal or quasi-thermal Comptonization models are favored (e.g., Sunyaev & Titarchuck 1980; Haardt & Maraschi 1991, 1993, hereinafter HM91 and HM93, respectively; Ghisellini, Haardt, & Fabian 1993; Titarchuck & Mastichiadis 1994; Zdziarski et al. 1994, 1995; see Svensson 1996 for a recent review).

The origin of the Comptonizing electrons is at present unknown. They could be related to an accretion disk corona heated by magnetic dissipation processes, and/or they may be electron-positron pairs produced by photon-photon collisions (see, e.g., Fabian 1994, and references therein). The electron temperature can be constrained by a thermal balance equation, where the heating rate is the total (direct plus reprocessed) luminosity and the cooling mechanism is Comptonization of soft photons.

The hot corona is probably coupled to a cooler optically thick gas layer (presumably the accretion disk itself), which has three major roles: (1) it reprocesses a fixed fraction of the Comptonized radiation into a soft blackbody component; (2) a fixed fraction of the reprocessed blackbody photons crosses the hot region, acting as seed photons for the Comptonization process; (3) it reflects medium-energy X-rays, giving rise to the so-called reflection component and Fe line emission. This picture (HM91; HM93) is suggested by the presence of the Compton reflection hump (Pounds et al. 1990) and by the relatively small dispersion in the distribution of spectral indices of Seyfert 1 galaxies (Nandra & Pounds 1994). In fact, if X-ray reprocessing contributes soft photons proportionately to the medium–hard X-ray luminosity, the "feedback" effect keeps a quasi-constant X-ray spectral shape, weakly dependent on the source luminosity. The broadband spectra derived from this model are consis-

[1] Institute for Theoretical Physics, University of California at Santa Barbara, Santa Barbara, CA 93106.
[2] Present address: Università degli Studi di Milano, 20133 Milano, Italy.

tent with the average Seyfert spectrum derived from OSSE observations (Zdziarski et al. 1995; Gondek et al. 1996).

It is fair to point out that the best studied object, NGC 4151, shows (at least in low state) an unusually flat X-ray spectral index ($\alpha \simeq 0.5$) and a low temperature ($kT \simeq 60$ keV) implying a Comptonized-to-thermal luminosity ratio $L_C/L_s \gtrsim 10$, far from the limit $L_C/L_s \simeq 2$ obtained in a plane-parallel geometry. This may be accounted for by a special geometry, for instance, if the high-energy emission originates in localized nonplanar active blobs as in the model proposed by Haardt, Maraschi, & Ghisellini (1994; hereinafter HMG).

Alternative models involving a mirror reflection of the observed radiation (Poutanen et al. 1996) or reprocessing in clouds along the line of sight (Zdziarski & Magdziarz 1996) may also apply for this special object.

In Comptonization models the spectral shape in the X-ray range is mainly determined by the combination of the temperature $\Theta = kT/mc^2$ and the optical depth of the scattering electrons τ, while the cutoff energy is related essentially to Θ. Simultaneous measurements of the spectral index α and of the cutoff energy can therefore determine the physical parameters of the Comptonizing region.[3]

"Spectral dynamics," i.e., the variation of the spectral shape with intensity, is an additional basic diagnostic tool (see, e.g., Netzer, Turner, & George 1994) that can test the model and provide insight into the way the corona is heated and cooled. Some of the questions that could be answered are the following: Is the optical depth of the corona dominated by e^+e^- pairs? How do the optical depth and electron temperature vary with luminosity? Are the reprocessed components proportional to the Comptonized component during variations? For instance, a careful analysis of *EXOSAT* spectra of Seyfert galaxies showed that the observed spectral variability is difficult to reconcile with nonthermal pair models (Grandi, Done, & Urry 1994).

Another important prediction of the model is the presence of a thermal component that should be proportional to the Comptonized component in the limit of a constant geometry. Its temperature, however, is not completely constrained by the model and could range from UV to soft X-rays. The presence of a "soft excess" in the X-ray spectra of AGNs has been detected by different experiments (*EXOSAT*, *ROSAT*, and, more recently, *ASCA*) (e.g., Arnaud et al. 1985; Pounds et al. 1986; Wilkes & Elvis 1987; Turner & Pounds 1989; Elvis, Wilkes, & McDowell 1991; Comastri et al. 1991; Saxton et al. 1993; Walter & Fink 1993; Turner, George, & Mushotzky 1993; Brandt et al. 1994; Done et al. 1995). It has been interpreted in some cases as a genuine thermal component that is possibly due to reprocessing (see, e.g., Leighly et al. 1996) or as the high-energy tail of the UV bump (e.g., Walter & Fink 1993), while in other cases it is viewed as an artifact of the residuals that is due to incomplete absorption (warm absorber; see, e.g., Done et al. 1995). Instruments with improved energy resolution in the soft band are needed to clarify the interpretation of the "soft excess" that may even involve more than one component. However, a distinctive point between different models is the predicted correlation between the soft and medium X-ray intensities. On this aspect of the problem useful data obtained from extensive observations of some Seyfert galaxies with *ROSAT* and/or *ASCA* already exist, and more will surely become available in the near future.

We are therefore motivated to examine in detail the broadband spectral variability expected in the accretion disk with hot corona model developed in previous papers (HM91; HM93; HMG). We will concentrate on extragalactic objects such as Seyfert 1 galaxies. The issue is complicated for several reasons. A quantitative analysis requires spectral simulations since "second-order effects" are important (see § 3). However, the main uncertainty is our poor knowledge of the physics of the corona. For instance, do the active coronal regions vary in size and/or height above the reprocessing disk? And how is the heating rate related to the optical depth?

In the following we chose the simple case in which the active and reprocessing region(s) can vary in area but maintain a fixed ratio between Comptonized and soft cooling photons. In particular, we choose the limit of a plane-parallel geometry characterized by a Comptonized-to-soft ratio $L_C/L_s \simeq 2$. This is not inconsistent with an inhomogeneous picture in which each active region can be approximated as being plane parallel. With these restrictions we compute explicitly the expected relations between "observable quantities," e.g., the variation of the 2–10 keV spectral index (including reflection) with temperature and intensity, and the variation of the soft intensity "S" (0.1–2 keV) with medium "M" (2–10 keV) and hard "H" ($E \gtrsim 30$ keV) intensity.

The plan of this paper is as follows. In § 2 we describe the model and the methods used for the computation of the spectra and for the derivation of the "observable" quantities. Since the key parameter driving spectral variability in the medium band is τ, while spectral variability in the soft band is essentially related to T_{BB}, we found it convenient to discuss relations between spectral and flux variability in the two bands separately. For this reason, in § 3 we deal with the expected spectral variability in the medium and hard X-ray bands, using the 2–10 keV spectral index, the 2–10 keV intensity, the temperature of the hot corona, and the 30–100 keV intensity, while in § 4 we compute the intensity and spectral variations of the soft reprocessed blackbody component for different variations of the system parameters. The results are converted into count rates and hardness ratios in the 0.1–0.4 and 0.9–2 keV bands using the *ROSAT* response matrix and a standard neutral hydrogen column. We discuss the expected correlations between variability in the soft and medium energy bands and compare the results to available observations in § 5. An exhaustive summary and final conclusions are presented in § 6.

2. THE DISK-CORONA MODEL

We follow a scenario originally proposed by Liang (1979), and revived by HM91 and HM93, in which the accretion flow is illuminated by the hard X-ray source (as the observed reflection spectrum indicates). A large fraction (about 80%–90%) of the incident power is expected to be thermalized in the disk and reemitted as thermal reprocessed radiation, which is in turn Comptonized in the

[3] The exact relation between α and τ depends on the geometry of the scattering region. The optical depth can therefore be deducted from observations only "modulo geometry." On the other hand, fitting the data assuming a simple homogeneous sphere gives a value of τ that is also a good estimate of the average (over all directions) scattering optical depth for any other possible geometry.

corona producing the X-rays. If the reprocessed radiation energy density dominates over the local disk thermal emission, the Compton y parameter is forced to be $\simeq 1$ independently of the coronal scattering opacity. This in turn ensures that the Comptonized radiation exhibits a spectral index close to 1. One possible configuration that satisfies the above condition is a plane-parallel corona above an accretion disk. In this case the condition $y \simeq 1$ is achieved only if the *entire* available gravitational power is released in the hot corona. In this case the *reprocessed thermalized* radiation coincides with the UV bump, and the *reprocessed reflected* radiation forms the 30 keV Compton hump.

The same condition can be satisfied if there are several such smaller regions above the disk, rather than a single smooth corona (HMG). In the latter case only a fraction of the available energy needs to be released in the hot corona. However, being localized in hot spots, the reprocessed thermalized radiation can still dominate the cooling. The underlying accretion disk can contribute to most or at least part of the total luminosity in the UV band as in the standard Shakura-Sunyaev disk model (Shakura & Sunyaev 1973). As in the uniform corona case, the *reprocessed reflected* radiation forms the 30 keV Compton hump, while the *reprocessed thermalized* radiation is probably emitted in hot spots in the EUV–soft X-ray band (HMG). Therefore, the emission in the EUV–soft X-ray band should be closely connected to the hard X-ray radiation.

In the present paper we assume that the cooling time of the electrons in the corona is shorter than the timescale of variation of the heating rate, so that we can consider spectral and flux variability as a succession of stationary states. The Comptonized spectra are computed in plane-parallel geometry for different inclination angles ϑ. A quadrature scheme was implemented to solve the radiation field for successive scattering orders, taking into account anisotropic Compton emission for the first scattering distribution (Haardt 1993). The single-scattering photon distribution is computed by means of the fully relativistic kernel for isotropic unpolarized radiation (Coppi & Blandford 1990). This ensures that the exponential rollover of the spectrum is correctly modeled as we tested against Monte Carlo calculations. The present numerical spectra are therefore in much closer agreement with recent detailed calculations by Poutanen & Svensson (1996) than the approximated treatment of HM93. An extensive discussion of the method we used can be found in Haardt (1994).

The downward Compton flux (i.e., the X-ray flux leaving the corona with an angle $\vartheta > \pi/2$) is averaged over the solid angle and then reflected by an infinite neutral layer (which mimics the accretion disk) with solar metal abundances. The angular distribution of the reflected spectrum is computed in the approximated way described in Ghisellini, Haardt, & Matt (1994) (see Burigana 1995 and Magdziarz & Zdziarski 1995 for detailed calculations). The angle-dependent reflected spectrum is then Comptonized in the corona and added to the primary continuum. The "measurable" spectral index in the [2–10] keV band is obtained by fitting with a power law to the composite spectrum and disregarding the goodness of the fit. The photon flux (i.e., number of photons per unit time per unit surface) in interesting bands is readily obtained by integration over energy.

Concerning the soft photon input, we consider cases in which the reprocessed radiation is isothermal and has a temperature $T_{\rm BB}$ between 10 and 300 eV. This scenario can be regarded as a uniform corona located above the very inner part of the accretion disk or, alternatively, as a blobby structure in which the overall X-ray emission is dominated by few blobs with similar properties.

With our approximations the interesting quantities can be computed with good accuracy and quickly. A more detailed treatment of the full radiative transfer problem in the same context, including free-free radiation, double Compton scattering, detailed pair balance, and polarized scattering, can be found in Poutanen & Svensson (1996).

3. VARIABILITY IN THE MEDIUM AND HARD X-RAY DOMAINS

3.1. *The α-τ Relation*

Since the model constrains the Compton parameter to be almost constant, one expects that the spectral index of the Comptonized spectrum is fairly constant, too, and does not depend on the three parameters of the system (i.e., τ, Θ, and $T_{\rm BB}$).

The above argument is valid, however, only as a first-order approximation, in particular, in the case of a disk-corona system, where the scattering anisotropy is important and when we consider the actually observed spectrum that includes the reflection hump. We therefore computed the spectral index of the *total* spectrum in the [2–10] keV range $\alpha_{[2-10]}$ as described in the previous section for different values of the coronal parameters and of the inclination angle. Comptonization of the reflected spectrum is also included.

The results are shown in Figures 1 and 2, where $\alpha_{[2-10]}$ is plotted versus the optical depth and the temperature of the corona, respectively, for two values of the inclination angle and two values of the temperature of the soft photons. In order to show the effect of reflection on the total spectrum, in Figure 3 we plotted, as a function of τ, the difference between the spectral index of the intrinsic continuum alone and that of the total spectrum (continuum + reflection).

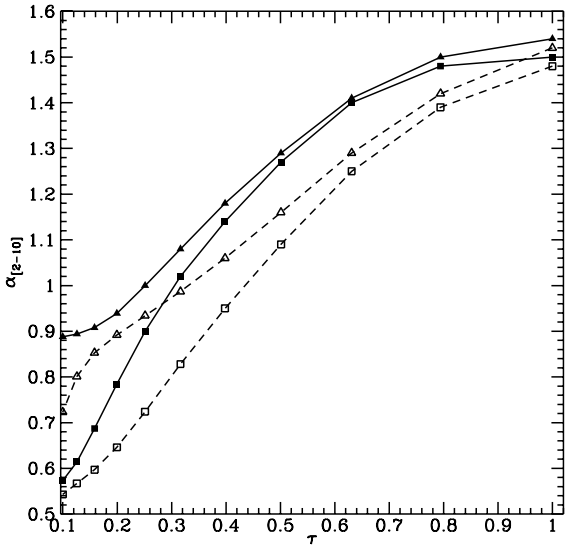

FIG. 1.—Total (direct power law + Comptonized reflection) spectral index in the [2–10] keV range $\alpha_{[2-10]}$ is plotted against the coronal scattering optical depth τ. Open symbols connected by dashed lines refer to spectra computed with $kT_{\rm BB} = 100$ eV. Closed symbols connected by solid lines are for $kT_{\rm BB} = 50$ eV. Squares indicate that a face-on line of sight is assumed, and triangles signify a 60° inclination.

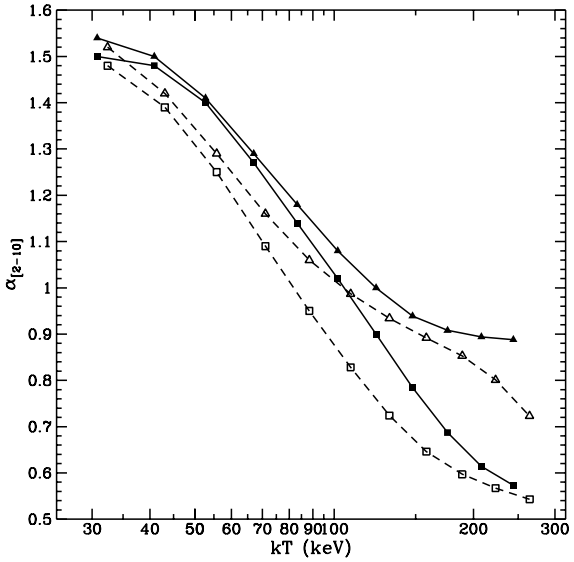

FIG. 2.—Total (direct power law + Comptonized reflection) spectral index in the [2–10] keV range $\alpha_{[2-10]}$ is plotted against the coronal electron temperature kT. Symbols as in Fig. 1.

The optical depth was varied between 0.1 and 1, corresponding to an equilibrium temperature of the hot corona in the range 30–300 keV, as suggested by observations (Maisak et al. 1993; Johnson et al. 1993; Madejski et al. 1995).

The important points to note are the following:

1. Changes in τ give rise to significant spectral variability despite the fact that the ratio L_C/L_s is constant in the model. In the plane-parallel limit considered here $\alpha_{[2-10]}$ is found to be in the range [0.5–1.5] for τ varying between 0.1 and 1.

2. Steeper spectra are produced as τ increases approaching unity.

3. An increase of the spectral index is accompanied by a decrease of the coronal temperature, i.e., *spectral index and coronal temperature are anticorrelated*. The actual values of α and kT in Figure 2 refer to $L_C/L_s \simeq 2$; however, the anticorrelation between spectral index and the electron temperature is a general feature common to models based on Compton cooling with fixed L_C/L_s. For higher values of L_C/L_s a similar curve would be obtained, but with values of α shifted downward. As shown in Figure 2, the dispersion of the $\alpha_{[2-10]}$ versus kT relation is larger at higher temperature.

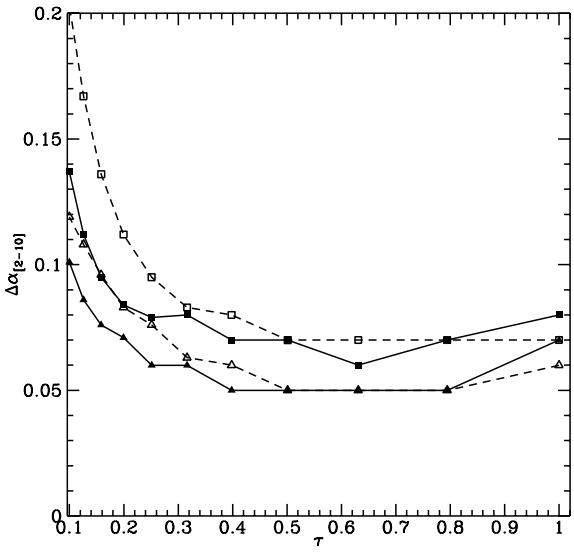

FIG. 3.—Difference between the spectral index of the [2–10] keV intrinsic continuum and that of the [2–10] keV total spectrum (continuum + reflection) is plotted vs. the optical depth τ. Symbols as in Fig. 1.

A physical understanding of these results involves several effects:

1. For any given τ the temperature has to adjust to maintain an almost fixed ratio L_C/L_s, and for increasing τ the temperature decreases. The resulting average spectral index (i.e., the spectral index averaged over the total solid angle) is, for the plane-parallel geometry adopted here, slightly larger than 1 for any value of τ (HM93). Comptonization theory implies that, in order to keep a constant ratio L_C/L_s, a spectral index *steeper than 1* must increase with decreasing Θ (i.e., increasing τ). This can be understood by noticing that the extrapolation to low energy of the Compton power law must intercept the peak of the *injected* blackbody soft photon distribution. Since for $\alpha > 1$ the integral over the energy of the power-law spectrum mainly depends on the lower integration limit $E_1 \propto (16\Theta^2 + 4\Theta + 1)kT_{BB}$, a shift to lower energy of E_1 (i.e., a decrease of Θ) keeping α constant would result in a larger ratio L_C/L_s. Therefore, in order to keep the ratio constant, the spectral index is forced to steepen (for the same reason, if $\alpha < 1$, a reduction of Θ implies a further *flattening*, rather than a steepening, of α). The steepening of α halts when a further decrease of Θ does not cause a shift of E_1 to lower energy, i.e., when $16\Theta^2 + 4\Theta \ll 1$, say $16\Theta^2 + 4\Theta \lesssim 0.5$. For even smaller temperatures the spectral index must *flatten* (and hence there is a maximum in the α vs. Θ curve) since, although E_1 is constant, the upper integration limit ($\propto\Theta$) decreases anyway. In terms of τ, since in our adopted geometry the Compton parameter $y \simeq (16\Theta^2 + 4\Theta)\tau$ is $\simeq 0.6$ (HM93; Poutanen & Svensson 1996), the "turning point" occurs for $\tau \simeq 1$. Note that for $\alpha < 1$ ($L_C/L_s \gtrsim 2$) there is a monotonic flattening of α as Θ decreases. The effect discussed here is independent of the particular geometry adopted. In brief, a fixed L_C/L_s ratio does not imply an exactly constant spectral index (e.g., see Fig. 2 in Ghisellini & Haardt [1994; hereinafter GH94] for the simplest possible geometry, i.e. a homogeneous spherical source, where this effect is present).

2. The outgoing Compton spectrum in plane-parallel geometry is a function of the emission angle because of the Compton rocket effect (Haardt 1993). Flatter spectra are seen for lower inclinations, and the importance of the anisotropic Compton emission decreases with decreasing coronal temperatures. Anisotropic Compton emission is the main cause of the reduction of $\alpha_{[2-10]}$ for small τ. This effect goes in the same direction as that discussed in point 1 above but, contrary to it, depends on the adopted geometry (e.g., it is absent in GH94). The larger dispersion of the $\alpha_{[2-10]}$ versus kT relation at high temperature (see Fig. 2) is due to the increasing importance of anisotropic Compton emission for increasing kT (see Haardt 1993 for details).

3. The contribution of the reflected Compton hump to the emitted spectrum is $\propto e^{-\tau/\mu}$, where μ is the cosine of the inclination angle, so it is smaller for larger τ (for fixed inclination angle) and can be boosted by anisotropic Compton

scattering (HM93) for high temperatures. As long as $\tau \gtrsim 0.4$, the contribution of reflection to the [2–10] spectrum is marginal ($\Delta\alpha_{[2-10]} \simeq 0.05$–$0.08$). For lower τ the electron temperature is high enough for anisotropic Comptonization to boost reflection. The effect, for fixed τ, is larger for larger μ and larger kT_{BB} (see Fig. 3). Again, this is an effect for which the net result is to flatten the total spectrum as τ decreases.

4. Finally, we discuss the effect on α of a change in T_{BB}. In fact, the Compton y parameter depends not only on L_C/L_s but also (only weakly when $y \lesssim 1$) on the mean energy of the soft photons. This can be easily understood by considering that the higher the energy of the soft photons injected in the corona, the lower the number of scatterings needed to reach an energy $\sim kT$. When $y \ll 1$ the (low) cooling is due only to the first scattering, so that $L_C/L_s \simeq y$. The relation between L_C/L_s and y does not depend on any other parameter, but as soon as y increases higher order scatterings become important in the cooling process. The asymptotic limit for $y \gg 1$, i.e., when all the photons reached thermal equilibrium, is $L_C/L_s = 4\Theta/x_0$, where x_0 is the dimensionless soft photon mean energy $\simeq 2.7kT_{BB}/mc^2$. For this reason, for a given τ the equilibrium temperature necessary to sustain a given L_C/L_s is (only slightly for $y \simeq 1$) higher (and hence the Compton spectrum flatter) for higher T_{BB} (for a visualization of how y varies with T_{BB} see Fig. 1 in Shapiro, Lightman, & Eardly 1976). Large changes in T_{BB}, unlikely to occur in a given source, are required to produce significant changes in α. However, this effect could be relevant when comparing different classes of sources (e.g., Seyferts and QSOs) where the difference between the average values of T_{BB} can be large enough to influence the value of the spectral index of the hard X-rays. As we will discuss in § 4, variations of T_{BB} in a particular object, even if small, can play an important role in the observed variability in the soft X-ray band.

As discussed in § 2, $\alpha_{[2-10]}$ is a simple least-squares fit to the total spectrum, which is not a perfect power law (because of, e.g., anisotropy and inclusion of reflection). In order to quantify the differences between the computed spectra and a power law, we associated a fixed percentage error to each of our 10 computed spectral points. By varying the error until a reduced χ^2 of unity was obtained in the least-square fits, we estimated a minimum observational precision required to detect the spectral distortions. For the most distorted spectra (those at low inclination and low τ) an observational error $\lesssim 2\%$ would result in a reduced χ^2 larger than unity. The typical maximum error allowed is $\lesssim 1\%$.

We now discuss the relation between $\alpha_{[2-10]}$ and the X-ray luminosity L_C on the basis of two alternative limits. The first case corresponds to a pair-dominated corona where the optical depth is determined by the compactness. In the second case the relation between τ and L_C is essentially unknown, and we will consider the limit case in which τ varies with constant luminosity.

3.2. *The α-Flux Relation in a Pair-dominated Corona*

If the corona is pair dominated, which is plausible in the case of compactness $l_C \gtrsim 10$, where $l_C = (L_C/R)(\sigma_T/m_e c^3)$ and R is the typical size scale of the emitting region (see Svensson 1996 for an exact definition of compactness in different geometries), the optical depth of the hot phase is determined by the compactness alone. As discussed in HM91, once the ratio L_C/L_s and the absolute value of l_C are specified, there exists a univocal correspondence of these parameters with τ, on the assumption that pairs dominate the scattering opacity over normal plasma. Thus, if variations of the compactness are due to variations of the dissipated luminosity L_C, the optical depth and hence the actual value of $\alpha_{[2-10]}$, depend on the intensity of the source.[4]

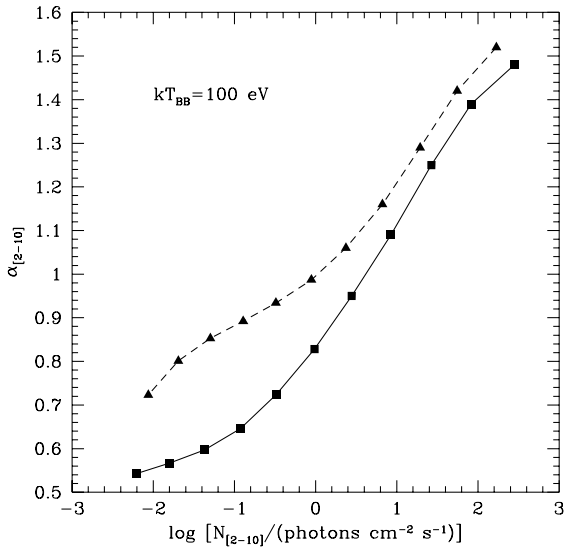

FIG. 4.—Total spectral index $\alpha_{[2-10]}$ is plotted vs. the photon flux in the [2–10] keV band (arbitrary normalized) in the case of a pair-dominated corona. Squares connected by a solid line refer to a case with a face-on line of sight, and triangles connected by a dashed line to an inclination of 60°. $kT_{BB} = 100$ eV in both cases.

From the $\alpha_{[2-10]}$ versus τ relation computed previously (Fig. 1) we can therefore derive for a pair-dominated corona an $\alpha_{[2-10]}$ versus intensity relation. This is shown in Figure 4 for two values of the viewing angle. It is quite clear (see also Fig. 2 in Stern et al. 1995) that noticeable variations of $\alpha_{[2-10]}$ (say $\Delta\alpha_{[2-10]} \simeq 0.3$) occur as the luminosity (and hence the compactness) varies by at least a factor of 20. Thus *for a pair-dominated corona the spectral index must be essentially constant during "normal" AGN X-ray variability (i.e., flux variations within a factor of 2 or so)*. Modest spectral steepening can occur during very large intensity increases.

On the other hand, spectral steepening also implies a decrease of the coronal temperature (Fig. 2) (see also Pietrini & Krolik 1995). Since an observational determination of the latter with the instrumentation available at present is not easy, we also computed the variation in the hard photon intensity ([30–100] keV) that would be associated with a variation in the [2–10] keV intensity. This is shown in Figure 5, where we also report values of $\alpha_{[2-10]}$ corresponding to different values of the intensity. The two intensity scales are arbitrary, but their ratio is not. As a result of the temperature decrease for increasing luminosity, the intensity in the hard band varies less than that in the medium band. However, the two are positively correlated.

[4] Stern et al. (1995), and more recently Poutanen & Svensson (1996) and Svensson (1996), pointed out that the exact relation between the rate of pair production and the heating and cooling rates depends on the details of the calculations. We have taken the compactness vs. τ curve given by Svensson (1996) in order to compute the photon flux in the [2–10] keV band.

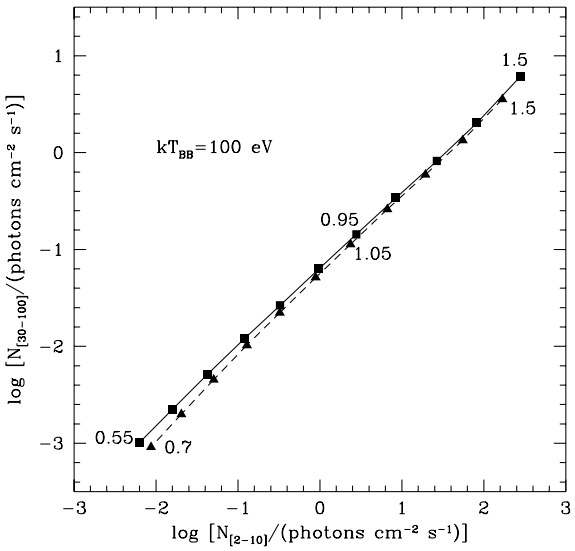

FIG. 5.—The photon flux in the [30–100] keV band is plotted vs. the photon flux in the [2–10] keV band in the case of a pair-dominated corona. Normalization is arbitrary. Curves are for $kT_{BB} = 100$ eV; squares indicate a face-on line of sight, and triangles signify a 60° inclination. The value of the total spectral index $\alpha_{[2-10]}$ in the [2–10] keV range is indicated for some of the spectra.

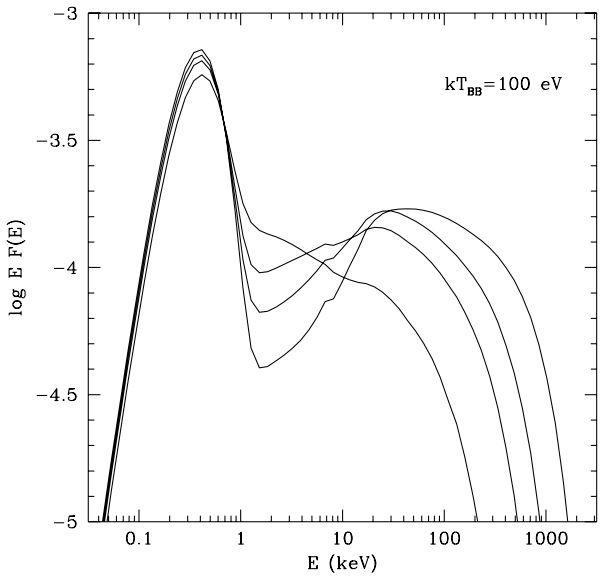

FIG. 6.—Comptonized spectra for different values of (τ, Θ) equilibrium values [(0.63, 0.11), (0.32, 0.21), (0.2, 0.3), (0.1, 0.5)]. kT_{BB} is set to 100 eV, and a face-on line of sight is considered.

Because of the large overall luminosity variation, the steeper and cooler spectrum does not cross the flatter, hotter one except at very high energy.

Different conclusions hold if variations of l_C are due to variations of the linear dimension of the source R rather than to variations of the intrinsic luminosity. Such a circumstance can occur if the corona is formed by many active regions rather than being homogeneous. In this case significant spectral variations could occur without large variations in the output. Strong effects on the soft X-ray spectrum are expected since the temperature of the reprocessed radiation scales as $1/R^2$. A detailed discussion will be presented in § 4.

3.3. *The α-Flux Relation in a Low Pair Density Corona*

If the compactness is $\lesssim 10$, the corresponding pair optical depth is $\lesssim 0.1$ (Stern et al. 1995). The main contribution to the optical depth then comes from "normal" electrons, the number of which is not related to the source luminosity in a simple and easily predictable way. We therefore consider the case in which the optical depth changes while the dissipated luminosity does not vary substantially.

In Figure 6 we show the total spectra for some choices of input parameters. It is evident from the figure that, despite the fact that the total luminosity in the spectra is the same (when integrated over all the emission angles), the flux in the [2–10] keV band varies. The spectral index versus the photon flux in the [2–10] keV band is shown in Figure 7. We can see that small observed variations of the count rate can be accompanied by significant spectral variations. Another important result, only weakly dependent on details, is that as long as $\alpha_{[2-10]} \lesssim 1$, it correlates to the photon flux, i.e., the spectrum softens with increasing intensity, while for steeper spectra the two quantities are anticorrelated.

From Figure 6 it is also evident that the flux above 50 keV will decrease for increasing spectral index. The decrement is relatively modest as long as $\alpha_{[2-10]} \lesssim 1$ since most of the power is carried by the few high-energy photons, but it becomes large as $\alpha_{[2-10]} \gtrsim 1$. Combining the spectral index intensity relation shown in Figure 7 with the spectral index temperature relation, we can compute the intensity in the hard X-ray band ([30–100] keV) versus the [2–10] keV intensity. This is shown in Figure 8. For $\alpha_{[2-10]} \gtrsim 1$ the emission in the [2–10] keV band is positively correlated with the emission in the γ-ray band: small increments in the X-ray flux are accompanied by larger increments in the γ-ray flux. For $\alpha_{[2-10]} \lesssim 1$ the correlation is in the opposite sense and is less strong: small increments in the medium X-ray emission relate to small decrements of the flux in the γ-ray band. Around the turning point $\alpha \simeq 1$ we have the largest variation of the γ-ray flux for the smallest variation of the X-ray flux.

In brief, the model predicts that if noticeable spectral variability is observed while the luminosity variation is less

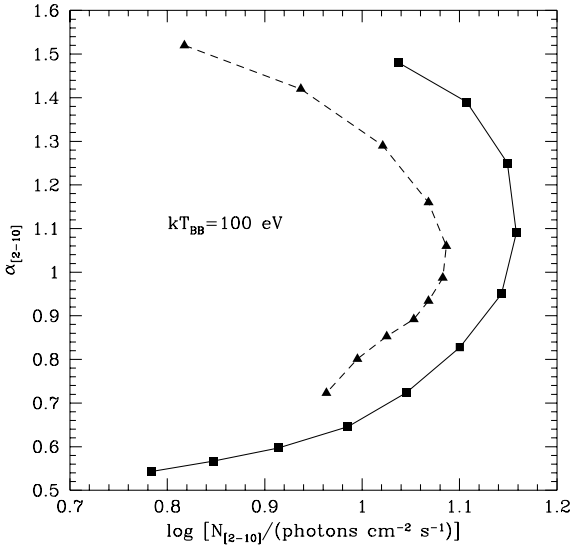

FIG. 7.—Same as Fig. 4, but in the case of τ variations with constant luminosity. Squares connected by solid lines are for a face-on line of sight, and triangles connected by dashed lines for a 60° inclination.

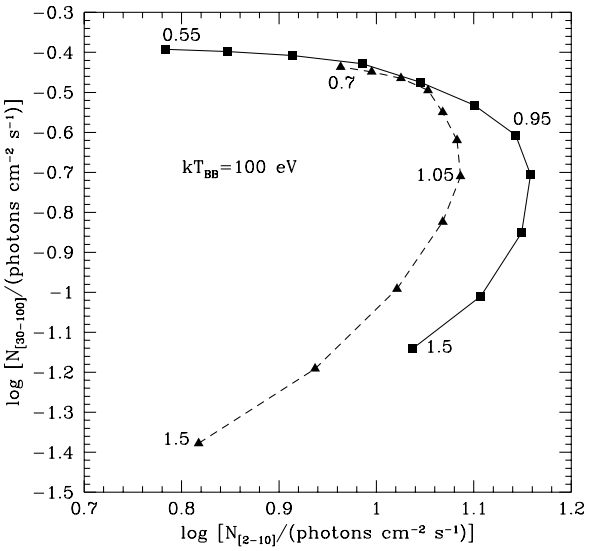

FIG. 8.—Same as Fig. 5, but in the case of τ variations with constant luminosity. Squares connected by solid lines indicate a face-on line of sight, and triangles connected by dashed lines a 60° inclination.

than factor of ~ 2, then *the scattering optical depth of the corona is not* (*or weakly*) *related to the intrinsic coronal luminosity*. This may lead to two possible conclusions:

1. Pairs are *not* important as a source of scattering material.
2. If pairs dominate the opacity, the linear dimensions of the source *must* vary; i.e., the compactness varies while the luminosity stays approximately constant.

In the latter case the temperature of the soft reprocessed photons must vary, increasing when the medium-energy X-ray spectrum steepens. In any case, strong spectral variability can well occur during "normal" (within a factor of 2) flux variations.

We caution here that in order to measure a variation in luminosity one should measure the intensity up to the high-frequency cutoff, that is, up to the 100 keV range. In the absence of such information one can *estimate* the luminosity variation from the known medium-energy intensity and the expected high-energy cutoff.

4. VARIABILITY IN THE SOFT X-RAY DOMAIN AND CORRELATIONS TO THE MEDIUM BAND

One of the basic features of the model is that a fraction of the Comptonized X-rays is reprocessed into soft thermal photons, which are in turn responsible for the cooling of the corona. This fraction is fixed for fixed geometry; therefore, the model predicts a "perfect" correlation between the Comptonized luminosity and the soft reprocessed one. Observationally, the latter component could be identified with the soft excess observed in Seyfert galaxies, although there is no general consensus on the very nature of the soft component. The soft X-ray emission has been identified as the high-energy tail of the UV bump (Walter & Fink 1993), but this claim and, in general, whether or not the soft X-rays are correlated to the UV emission is still controversial (see, e.g., Laor et al. 1994; Ulrich-Demoulin & Molendi 1996a, 1996b). The low *ROSAT* PSPC energy resolution does not allow us to constrain the spectral shape of the excess, and usually a steep power law is fairly adequate to fit the data (Gondhalekar, Rouillon-Foley, & Kellet 1996). Higher resolution *ASCA* data seem to support a thermal origin of this component (e.g., Leighly et al. 1996), although absorption features which are due to highly ionized gas along the AGN line of sight could be responsible for (at least of part) of the excess of residuals in the single power-law fits (e.g., Cappi et al. 1996). Indeed, some recent *ASCA* data are consistent either with an *emission* thermal component or with *absorption* which are due to highly ionized gas (IC 4329A, Cappi et al. 1996; NGC 3227, Ptak et al. 1995). In several objects both a warm absorber *and* a thermal emission component seem to be present (NGC 5548, Done et al. 1995; NGC 4051, Guainazzi et al. 1995; see also Netzer, Turner, & George 1994). Mathur, Elvis, & Wilkes (1995) argued that a highly ionized, high-velocity outflowing gas responsible for X-ray and UV absorption might be a common component in quasars and should be located outside the broad emission line region.

At least for NGC 5548 there are indications that the soft emission and the power law vary in a correlated fashion, but the correlation is nonlinear; i.e., the soft component varies more (Nandra et al. 1993; Done et al. 1995). In one case a 30% increase of the soft counts observed with *ROSAT* was not accompanied by a significant variation in the estimated power-law component. This event suggested that at least soft X-ray "flares" may well have a different origin than reprocessing of hard X-rays (Done et al. 1995).

We wish to stress here that the behavior of the observed soft X-ray intensity depends strongly on the spectrum, i.e. the temperature of the reprocessed emission T_{BB}. The latter depends on the absolute luminosity of the X-ray emission (we recall that in the model it equals roughly half of the total power produced via Comptonization) and on the size of the radiating surface. Unfortunately we do not know whether and how these two quantities are related with each other. As a first guess we may expect that both R and L scale with the mass of the source. This may determine a mean value of L/R^2 for a given source (sources with smaller masses would have hotter soft components); however, how the ratio varies when the luminosity varies in a given source remains highly unpredictable. Furthermore, the amplitude of variations in fixed energy bands can be different; e.g., the hardness ratios can change substantially when the response of a particular detector is considered. Comparison with observations can then be made by only "filtering" simulated light curves through the actual response matrix of existing experiments.

In brief, although there is a one-to-one correspondence between the Comptonized and reprocessed emission, this holds on global scale, i.e., considering the integrated total luminosities. What is actually observed as a "count rate" in the given bands can be very different from what is expected on this simple basis. In the following we compute the expected behavior of the soft X-ray intensity in response to variations of the medium-energy intensity in two limiting cases, for varying luminosity and fixed size of the reprocessing region and for constant luminosity and varying size. Since most of the observational data available at present derive from *ROSAT*, we explicitly compute intensities and hardness ratios in the most commonly used *ROSAT* bands.

4.1. *Simulated ROSAT Light Curves*

We performed simulations of variability patterns according to selected rules that will be described in the following. The time-dependent broadband spectra were then filtered

through a Galactic neutral absorber assuming $N_H = 2 \times 10^{20}$ cm^{-2} and were folded with the *ROSAT* response matrix. We divided the *ROSAT* band in three intervals, defining a "hard count rate" as the count rate in the [0.9–2] keV band ($C_{[0.9-2]}$; it should be kept in mind that in all the other sections the "hard" band refers to energies $\gtrsim 30$ keV) and a "soft count rate" as the count rate in the [0.1–0.4] keV band ($C_{[0.1-0.4]}$). We then computed the hardness ratio defined as HR $= C_{[0.9-2]}/C_{[0.1-0.4]}$. This quantity provides direct spectral information in the *ROSAT* range.

It is important to realize that the dependence of HR on the temperature of the soft component is not monotonic. This is shown in Figure 9*a* for two cases with regard to the power-law component (both with 0° inclination), one corresponding to low optical depth $\tau = 0.1$ (resulting in a flat spectral index $\alpha_{[2-10]} \simeq 0.5$–0.6; see Fig. 1), the second to higher optical depth $\tau = 0.65$ (yielding to $\alpha_{[2-10]} \simeq 1.2$–1.3) For a pair-dominated source these values of τ would imply a large difference in compactness, roughly 10^3 larger for the high τ case (see Svensson 1996). Intermediate cases must be included between the two curves. The relation is independent of the actual mechanism causing the variations of T_{BB} but depends somewhat on the parameters defining the hard power law.

The behavior of HR versus kT_{BB} is easily understandable. For low temperatures, only the exponential tail of the Planck distribution falls in the *ROSAT* band. In this regime a temperature increase leads to a large increase of the count rate in the soft band only: the spectrum becomes softer. The softening stops when the peak of the blackbody distribution is within the band, and the exponential tail starts to affect the intensity in the [0.9–2] keV band. In the latter regime when the temperature increases the spectrum becomes harder. The transition occurs for kT_{BB} around 60 eV.

In order to compute the relation between T_{BB} and the count rate in the *ROSAT* band, we have to specify the mechanisms leading to the temperature variations. We have considered two different ideal ways in which T_{BB} can vary, the first corresponding to variations in luminosity for fixed size, the second to variations in size for fixed luminosity, and discuss them in turn.

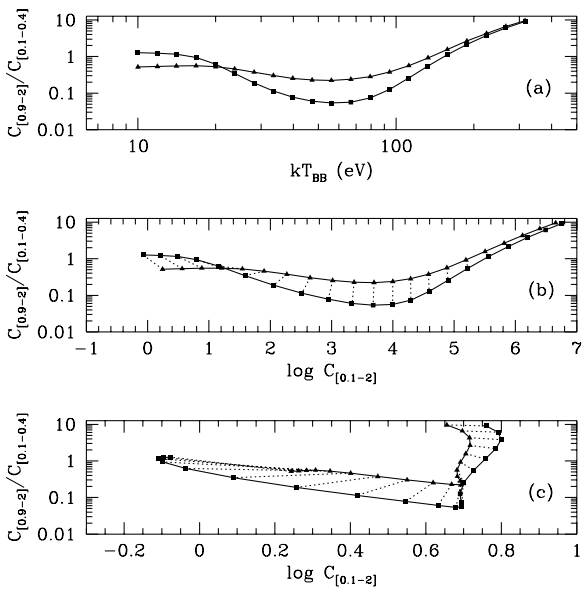

FIG. 9.—(*a*) Hardness ratio in the *ROSAT* band plotted vs. temperature of the reprocessed component. Squares refer to spectra computed with $\tau = 0.1, \Theta = 0.5$, while triangles with $\tau = 0.63, \Theta = 0.11$. (*b*) Hardness ratio is plotted vs. total count rate in the *ROSAT* band for a case of pure luminosity variations. Squares and triangles same as (*a*). Dashed lines connect spectra having equal kT_{BB}. (*c*) Same as (*b*), but for pure variations of the emitting area.

In all the cases discussed in this section the reprocessed thermal component is superimposed to a standard multicolor disk emission arising from a $10^7\ M_\odot$ black hole radiating at 10% of the Eddington limit. The X-ray luminosity is taken as 0.3 of the disk emission, and a face-on line of sight is assumed. We checked that our results are only marginally sensitive to disk parameters. For rather extreme cases such as a $10^6\ M_\odot$ black hole accretion disk radiating at the Eddington limit with an X-ray luminosity of only 10% of the UV disk emission, the *ROSAT* band is still dominated by the reprocessed X-rays as long as the temperature of the latter component is $\gtrsim 20$ eV. The net effect of increasing the inclination angle is to reduce the amplitude of variations of the count rate in the soft band.

4.2. *Variations of Intrinsic Luminosity*

Suppose the luminosity of the source in the power-law component changes (i.e., L_C changes), while τ and Θ remain constant. In this case an increase in luminosity produces an increase in temperature of the thermal component, and hence a correlation between medium and soft X-rays is expected.

The hardness ratio plotted in Figure 9*a* can now be plotted as a function of the intensity that would give rise to the considered temperature variation. This requires a very large intensity range, a factor 10^7 for kT_{BB} in the range 10–316 eV , implausible for the same source. Thus, a single source will be confined to some restricted interval in intensity, while different sources could fall in different regions of the plot. The results are shown in Figure 9*b*. The two curves correspond to the same coronal parameters used in Figure 9*a*. Clearly the count rate scale is arbitrary, but the absolute value of the hardness ratio is meaningful, being independent of the source luminosity for a given spectral shape. For reference, we plot along each curve discrete points corresponding to an increase in luminosity by a factor 2, i.e., to an increase of 20% in T_{BB} with respect to the preceding one. The exact value of kT_{BB} relative to each point can be easily read from Figure 9*a* where the same discrete points are marked.

The count rates in the two bands are always correlated, although the correlation is not linear. Even though the temperature only varies as $L^{1/4}$, as long as the temperature is $\lesssim 60$ eV, the number of soft photons emitted in the *ROSAT* band changes significantly for even modest variations of temperature. This regime corresponds to the decreasing branches of the curves in Figure 9*b*. Along this branch an increase in luminosity produces an exponential increase of $C_{[0.1-0.4]}$, while the increase of $C_{[0.9-2]}$ is linear, being dominated by power-law photons. The hardness ratio is clearly anticorrelated to the count rate. The total count rate shows large variations, being dominated by the lowest energy channels.

The behavior is very different when the peak of the blackbody spectrum is well within the *ROSAT* band, i.e., for $kT \gtrsim 60$ eV. The hardness ratio is constant as long as the exponential tail of the Planck distribution does not affect the [0.9–2] band. When this happens, $C_{[0.9-2]}$ responds exponentially to ΔL, while $C_{[0.1-0.4]}$ varies almost linearly.

The total count rate is almost linear with ΔL, so the spectrum becomes harder.

The case of a steep power-law component is qualitatively similar but less extreme. The variations of the hardness ratio are smaller in both branches.

In a pair-dominated source luminosity variations with constant coronal parameters are, strictly speaking, not allowed. States with different luminosity belong to curves with different values of τ. However, since the separation of the two curves for constant T_{BB} (*dotted lines*) corresponds to an increase of l_C of a factor $\simeq 10^3$, the shift corresponding to a factor 2 is clearly negligible.

4.3. *Variations of Linear Dimensions*

We consider the case of a constant output radiating from a varying surface area, while τ and Θ remain constant. This may represent a case in which the primary hard emission occurs at a constant rate in an expanding (and/or contracting) corona, or blob, or if the emission occurs at different time in blobs with roughly the same luminosity but different sizes.

Although the luminosity of the hard and soft components is constant, the temperature of the thermal photons will change, giving rise to observable effects in the soft X-ray domain. To study the problem we varied the linear size R of the emitting region, so that the resulting blackbody temperature covers the range 10–316 eV. Notice that under the assumption adopted, the intrinsic number of photons emitted scales as $R^{1/2}$, while the temperature varies as $1/R^{1/2}$. Therefore, the highest *intrinsic* photon emissivity occurs at the lowest temperatures. The relation between hardness ratio and count rates for constant luminosity and varying area is shown in Figure 9*c*. The two curves correspond to the same coronal parameters used in Figures 9*a* and 9*b*. The same discrete points plotted in Figures 9*a* and 9*b* are also marked, corresponding to a decrease of R of 30% (and hence resulting in an increase of T_{BB} of 20%) with respect to the preceding one.

The behavior of HR is similar to that seen in the previous section. As long as $kT_{BB} \lesssim 60$ eV, the soft counts increase, while the hard counts are much less variable. This regime corresponds to the decreasing branches of the curves in Figure 9*c*. Although HR is anticorrelated to the total count rate independently of the coronal parameters, the hard and soft count rates can be both correlated or anticorrelated, depending on whether the hard power law is steep or flat, respectively.

The behavior of HR versus the total count rate is very different when $kT_{BB} \gtrsim 60$ eV. Since the total luminosity is constant, the total count rate is basically constant when the peak of the blackbody distribution is within the *ROSAT* band. This regime corresponds to the almost vertical branches of the curves in Figure 9*c*: HR dramatically increases at almost constant total count rate. In this regime the peak of the blackbody spectrum moves from the soft band to the hard band. The net result is that the two count rates are anticorrelated: as T_{BB} increases, $C_{[0.9-2]}$ increases while $C_{[0.1-0.4]}$ decreases.

If the corona is pair dominated, variations of R should not occur with constant coronal parameters. A reduction in the radius by a factor $\simeq 10$ (which roughly corresponds to four successive points counting from left to right along the curves in Fig. 9*c*) causes an increase in the opacity and hence a reduction in the coronal temperature. For $kT_{BB} \lesssim 60$ eV the variations of HR will be smaller with respect to cases with constant τ and Θ. For larger values of kT_{BB} the situation is similar to what was seen before: a sharp increase of the hardness ratio with a constant count rate.

In the case of a low pair density corona described in § 3.2, the coronal parameters can vary without any change of size or luminosity of the soft component. In terms of *ROSAT* count rates, this is represented by the dashed lines in Figure 9*c*. Those lines connect points relative to spectra with different coronal parameters, but the same T_{BB} and luminosity. If, for example, an increase of τ occurs, the *ROSAT* count rate increases as long as $kT_{BB} \lesssim 60$ eV, slightly decreases for higher blackbody temperatures (Fig. 9*c*). The hardness ratio shows a slightly simpler behavior: for low temperatures it decreases and for $kT_{BB} \gtrsim 30$ eV it increases, tending to become constant at higher temperatures.

5. SPECTRAL AND FLUX CORRELATIONS: COMPARISON WITH OBSERVATIONS

We now compare the results discussed in the present sections with some of the current observations of soft and hard X-ray variability in Seyfert galaxies.

The two recently studied cases of NGC 5548 and Mrk 766 observed with *ROSAT* and/or *ASCA* provide the most detailed available information on spectral and flux variability of Seyfert 1 galaxies in the X-rays to date and also seem to indicate opposite behaviors. We should warn the reader that Mrk 766 is a rather extreme case, not representative of the Seyfert 1 class. Indeed, this source is classified as a narrow line Seyfert 1 (NLS1). Sources of this subclass tend to show rapid X-ray variability, unusually steep *ROSAT* spectra, and strong Fe II emission (Pounds & Brandt 1996).

We now compare those observations with the analysis developed in the previous sections. We do not aim to "fit" any data, but simply to interpret (whenever possible) the general variability features in the context of the reprocessing scenario.

5.1. *NGC 5548*

The soft X-ray variability of NGC 5548 observed by *ROSAT* has been deeply analyzed by Done et al. (1995). The soft and hard counts seem to go up and down together, but not in a linear way. In general, the source softens (in the *ROSAT* band) as it brightens. The hardness ratio roughly doubles (from 0.03 to 0.06) for a count reduction by a factor of 3. Also a state where only the counts in the *ROSAT* soft band varied was observed. No simultaneous observations in the hard X-rays are available. Old *GINGA* data showed a power-law index close to the canonical value 0.9 plus a reflection hump (Nandra & Pounds 1994).

The source requires a highly variable soft component and a more steady hard one. This can be roughly interpreted assuming that variability in the soft band is due to variations in size of the emitting area, as in the case discussed in § 4.3 (see Fig. 9*c*). The temperature of the thermal component should be less than 60–70 eV, which is not inconsistent with that found by Done et al. (1995). The intrinsic luminosity of the source should be roughly constant. We may notice that the lower value of the observed hardness ratio (0.03) is lower that the minimum value consistent with the reprocessing hypothesis (see Fig. 9). The discrepancy may be due to the value of N_H for this source ($N_H = 1.65 \times 10^{20}$ cm^{-2}; Done et al. 1995), which is lower than that used throughout our calculations ($N_H = 2 \times 10^{20}$ cm^{-2}),

but it may also indicate that part of the reprocessed thermal flux does not contribute to the cooling of the corona, or, alternatively, as suggested by Done et al. (1995), that there is another soft component unrelated to the hard one, possibly much broader than a single-temperature blackbody.

5.2. *Mrk 766*

Mrk 766 has been observed by *ROSAT* and *ASCA*, providing a full coverage of the X-ray domain from 0.1 to 10 keV. The *ROSAT* data have been analyzed by Molendi, Maccacaro, & Schaeidt (1993), Molendi & Maccacaro (1994), and recently by Leighly et al. (1996), who also analyzed the *ASCA* data. *ROSAT* data show that the source hardens as it brightens and can be roughly described by an almost steady soft component plus a variable hard one. In the *ASCA* band the source shows evidence of spectral variability above 1 keV ($\Delta\alpha \simeq 0.4$); the steepest state is brighter than the flat state in the *ASCA* band by a factor of $\simeq 2$. The power law pivots at an energy close to 10 keV. If the power law extends up to a few hundred keV, then the hard (and weaker in the *ASCA* band) state is actually more luminous than the soft state.

Observations indicate that $\alpha_{[1-10]}$ varies between 0.6 and 1, while the total luminosity changes by factor of 2 at most. This indicates that either pairs are not dominant or, if pairs dominate, that the linear size of the emitting region is varying. In the latter case the required change in compactness is roughly a factor 10. Since the overall X-ray luminosity of the hard state is estimated to be 2 times larger than that of the soft state (see below), the region responsible for the soft spectrum should be 20 times smaller than that responsible for the hard one. The soft state, although fainter by a factor 2, should then be characterized by $T_{\rm BB}$ roughly 3–4 times larger than that relative to the hard state. Data are consistent with a reduction of the excess normalization by a factor 2 as the power law steepens, but an increase of 3–4 times of $T_{\rm BB}$ in the soft state is not supported by the data.

We therefore conclude that the spectral variability in Mrk 766 could be due to changes of the scattering opacity of the corona without large variations of the intrinsic luminosity. The opacity of the corona is probably not dominated by electron-positron pairs. A variation of τ from $\simeq 0.3$–0.4 to $\simeq 0.1$–0.2 can explain the hardening of the power law and possibly (part of) the decrease in the *ASCA* count rate. We predict that the hard state is characterized by a coronal temperature $\simeq 150$–200 keV (and hence an exponential cutoff with an e-folding energy $E_C \simeq 300$–400 keV should be present), while the soft state should have $kT \simeq 80$–100 keV (corresponding to $E_C \simeq 150$–200 keV). The total X-ray luminosity of the hard state would then be 2 times larger than that of the soft state.

Finally, we note that the value of hardness ratio in the *ROSAT* band computed by Molendi & Maccacaro (1994) ranges from $\simeq 0.5$ to $\simeq 1$. According to Figure 9*a* this would imply a temperature of the soft component of $\simeq 130$ eV, in agreement with the observed hardening with increasing intensity in the *ROSAT* band and with the *ASCA* results.

6. SUMMARY AND DISCUSSION

6.1. *Summary*

We have examined the expected spectral variations within a model involving a hot corona emitting medium to hard X-rays by Comptonization, coupled to a cooler optically thick layer which (1) provides the input of soft photons for Comptonization by the hot corona and (2) intercepts a fixed fraction of the Comptonized photons and reprocesses them into soft thermal photons. The fraction of hard photons that are reprocessed and the fraction of soft photons that are Comptonized have been held fixed to the standard values of $\frac{1}{2}$ and 1, respectively, which refer to a flattened, sandwich-like geometry. These values may be somewhat different in different sources but could be constant on "short" timescales, over which the structure of the emitting region is not expected to vary substantially.

Even with these restrictions, the spectral variability is rather complex and depends on two main issues: the importance of pairs as a source of opacity, and the expansion/contraction of the active regions in the corona possibly associated with luminosity variations.

The main point that emerges is that intrinsic spectral variations are governed by changes in opacity (steeper spectra for larger τ as long as $\tau \lesssim 1$). For fixed L_C/L_s this implies that *a steepening of* α *should correspond to a decrease of the temperature*. This is a robust prediction of Compton-cooled models with fixed geometry and could be tested by the recently launched *XTE* and *SAX* satellites. Should an opposite behavior be found, the concept of a quasi-stationary corona above an accretion disk should be substantially revised in the sense of a much more chaotic situation.

The relation between spectral shape and intensity is univocal in the case of pair-dominated coronae. In this case large changes in compactness (luminosity and/or size) are required for modest spectral variations. These should appear as either large changes in the 2–10 keV intensity or large changes in the temperature of the soft reprocessed component. The case of Mrk 766 (which may be anomalous among Seyfert 1 galaxies) seems to exclude a pair-dominated corona.

In the case of negligible pairs the relation between luminosity and opacity is essentially unknown. Opacity variations could occur with little variations in luminosity and give rise to a pivoting of the medium-energy spectrum which can yield little correlation and even anticorrelation between the hard and medium X-ray fluxes. For constant luminosity and flat spectral indices ($\alpha_{[2-10]} \lesssim 1$) the hard photon flux varies less and is anticorrelated with the photon flux in the medium-energy band.

The integrated luminosity in the soft reprocessed emission is always proportional to the Comptonized luminosity. However, its contribution to the counts in the band between the galactic absorption cutoff and the carbon edge depends strongly on the temperature, which increases with increasing luminosity (for fixed size). This can give rise to anomalous observed behaviors with larger variations in the soft band than in the medium one.

6.2. *Discussion*

From a more observational point of view, it may be useful to discuss in more detail what can be deduced about the intrinsic properties of the source from a given set of "observables." To this end we indicate the [0.1–2] keV band as the "soft S band," the [2–10] keV band as the "medium M band," and the band above 30 keV as the "hard H band." We define four observable quantities describing the continuum variability of a source in the

X-ray domain: variation of the [2–10] keV spectral index $\Delta\alpha$, variation of the [0.1–2] keV count rate ΔS, variation of the [2–10] keV count rate ΔM, and variation of the hard count rate ΔH. The four quantities defined are in principle independent, and hence all the possible variability behaviors can be described by a combination of possibilities. We will examine the most interesting ones.

The main relevant property of an observed X-ray light curve is whether flux variability in the M band occurs keeping a constant spectral index, or, instead, if it is accompanied by spectral variations. The two possibilities, together with simultaneous observations in the S band, lead to very different conclusions regarding the very nature of the observed variability.

As discussed in § 3, spectral variations in the medium band require a negligible number of pairs in the corona or, for large compactness, variations of the source linear size R. Observations in the soft band can discriminate between the two possibilities since the latter case would imply variations of $T_{\rm BB}$ and hence variations of the soft counts. Hence, in case $\Delta S \simeq 0$ the intrinsic luminosity of the X-ray source and the dimensions of the reprocessing region must not vary; the hard variability in flux and spectral index is due to variations of optical depth of the corona, with a negligible contribution of pairs. The model predicts that $\alpha_{[2-10]}$, whenever steeper than 1, is anticorrelated to the medium count rate. A positive correlation holds if instead $\alpha_{[2-10]} \lesssim 1$. The temperature of the corona decreases for increasing spectral index, and the flux in the H band is correlated to that in medium band if $\alpha_{[2-10]} \gtrsim 1$ and is anticorrelated if $\alpha_{[2-10]} \lesssim 1$. The case with $\Delta S \neq 0$ is similar, but the observed variability properties can be due both to variations of the intrinsic luminosity of the corona and/or to variations of the linear size of the reprocessing region. If the corona is pair dominated, the model predicts that the soft-component temperature is correlated to $\alpha_{[2-10]}$ and is anticorrelated to Θ. In the case in which pairs are unimportant, it is not possible to draw any predictable relation between $\alpha_{[2-10]}$ and the medium or soft count rates. A full coverage through the X-rays to the γ-rays can determine in principle if the intrinsic luminosity of the source varies. In the case of negligible luminosity variations, changes in $T_{\rm BB}$ must occur to produce a nonnull ΔS. On the other hand, if intrinsic luminosity variations were detected, they alone could give raise to the observed variability in the soft band without associated variations of $T_{\rm BB}$. In principle, the nature of variability in the soft band (variations of intrinsic flux or variations of temperature) can be tested by high spectral resolution observations.

Different conclusions can be drawn if the variability in the medium band occurs with a constant spectral index. The main result is that the intrinsic luminosity of the source must vary, but not the properties of the hot corona. This can happen in a pair-dominated source if the variations of compactness are $\lesssim 2$. An observation of $\Delta M \gtrsim 10$ with a constant spectral index would imply that some mechanism different from pair balance works to keep the coronal optical depth constant. In any case, the model predicts that $\Delta S \neq 0$. The total counts in the soft and hard bands are positively correlated, and much stronger variations occur in the soft band than in the medium one. The quantity Θ should not vary noticeably, while the flux in H band follows the variations of the M band. If $\Delta S \simeq 0$, the model can be ruled out since any variation of the hard power law with a constant spectral index must be accompanied by an observable variation in the luminosity of the soft component. If this does not occur, the soft component cannot be due to local reprocessing of part of the hard X-rays.

It should be mentioned that, although the model considered in the paper constrains the ratio $L_{\rm C}/L_s$ to be constant ($\simeq 2$), in principle different behaviors are possible if instead the ratio $L_{\rm C}/L_s$ is allowed to vary. This can occur if the height-to-radius ratio of the scattering region(s) is of order unity or larger (see, e.g. , HMG and Stern et al. 1995). GH94 showed that in the case of a pair-dominated homogeneous plasma with $\Theta \lesssim 1$, an increase of $L_{\rm C}/L_s$ (and hence a decrease of α) would result in a lower temperature (and hence a relevant increase in τ must occur), contrary to the case of τ-driven spectral variations with constant $L_{\rm C}/L_s$. Thus, at least in principle, broadband observations could be used to check the stability of the Compton-to-soft ratio during spectral variations and, hence, the role played by reprocessing.

Finally, we wish to mention one aspect of the model neglected so far, namely time lags between different bands. In the most basic picture of Comptonization models, the hard X-rays respond to variations of the soft photon flux, and hence variations in the hard band should follow variations of the soft thermal photons, exhibiting also a steeper power spectrum (see, e.g., the discussion in Papadakis & Lawrence 1995). Data in this field are sparse and often contradictory (see Tagliaferri et al. 1996, and references therein). *EXOSAT* data of NGC 4051 seem to indicate that more power at high frequency is radiated by means of high-energy photons (Papadakis & Lawrence 1995), contrary to what is expected from the basic Comptonization theory.

The above considerations assume that spectral variability is due to variations of the primary soft photon input. In the model under investigation here, however, the soft photons are supposed to be generated by mere reprocessing of a fraction ($\simeq 50\%$) of the primary hard X-rays. Variations of the physical conditions occur primarily in the corona. For example, we may expect that a rapid variation of the heating rate appears in the Comptonized photons roughly at the same time at every energy, and eventually in the soft component. The situation appears to be extremely complicated, and we believe that the interpretation of data cannot avoid dealing with such complications (see, e.g., Nowak & Vaughan 1996). In view of forthcoming better timing data in a work in progress, we aim to perform a detailed analysis of the timing properties of an active Comptonizing corona.

F. H. wishes to thank S. Molendi for stimulating discussions and the Astrophysics Section of the University of Milan for hospitality. F. H. and G. G. thank the ITP in Santa Barbara where part of this study was carried out. F. H. acknowledges financial support by the Swedish Natural Science Research Council and by the Alice Wallembergs Foundation. This project was also partially supported (F. H. and G. G.) by NSF grant PHY 94-07194.

REFERENCES

Arnaud, K. A., et al. 1985, MNRAS, 217, 105
Brandt, W. N., Fabian, A. C., Nandra, K., Reynolds, C. S., & Brinkmann, S. 1994, MNRAS, 271, 958
Burigana, C. 1995, MNRAS, 272, 481
Cappi, M., Mihara, T., Matsuoka, M., Hayashida, K., Weaver, K. A., & Otani, C. 1996, ApJ, 458, 149
Comastri, A., Setti, G., Zamorani, G., Elvis, M., Giommi, P., Wilkes, B. J., & McDowell, J. C. 1991, ApJ, 384, 62
Coppi, P. S., & Blandford, R. D. 1990, MNRAS, 245, 453
Done, C., Pounds, K. A., Nandra, K., & Fabian, A. C. 1995, MNRAS, 275, 417
Elvis, M., Wilkes, B., & McDowell, J. C. 1991, in EUV Astronomy, ed. R. Malina & S. Bowyer (New York: Pergamon), 238
Fabian, A. C. 1994, ApJS, 92, 555
Ghisellini, G., & Haardt, F. 1994, ApJ, 429, L53 (GH94)
Ghisellini, G., Haardt, F., & Fabian, A. C. 1993, MNRAS, 263, L9
Ghisellini, G., Haardt, F., & Matt, G. 1994, MNRAS, 267, 743
Gondek, D., et al. 1996, MNRAS, submitted
Gondhalekar, P. M., Rouillon-Foley, C., & Kellet, B. J. 1996, MNRAS, 282, 117
Grandi, P., Done, C., & Urry, C. M. 1994, ApJ, 428, 599
Guainazzi, M., Mihara, T., Otani, C., & Matsuoka, M. 1996, PASJ, in press
Haardt, F. 1993, ApJ, 413, 680
———. 1994, Ph.D. thesis, ISAS/SISSA (Trieste)
Haardt, F., & Maraschi, L. 1991, ApJ, 380, L51 (HM91)
———. 1993, ApJ, 413, 507 (HM93)
Haardt, F., Maraschi, L., & Ghisellini, G. 1994, ApJ, 432, L95 (HMG)
Johnson, W. N., et al. 1993, A&AS, 97, 21
Laor, A., Fiore, F., Elvis, M., Wilkes, B. J., & McDowell, J. C. 1994, ApJ, 435, 611
Leighly, K. M., Mushotzky, R. F., Yaqoob, T., Kunyeda, H., & Edelson, R. 1996, ApJ, 469, 147
Liang, E. P. T. 1979, ApJ, 231, L111
Madejski, G. M., et al. 1995, ApJ, 438, 672
Magdziarz, P., & Zdziarski, A. A. 1995, MNRAS, 273, 837
Maisack, M., et al. 1993, ApJ, 407, L61
Mathur, S., Elvis, M., & Wilkes, B. 1995, ApJ, 452, 230
Molendi, S., & Maccacaro, T. 1994, A&A, 291, 420
Molendi, S., Maccacaro, T., & Schaeidt, S. 1993, A&A, 271, 18
Nandra, K., et al. 1993, MNRAS, 260, 504
Nandra, K., & Pounds, K. A. 1994, MNRAS, 268, 405
Netzer, H., Turner, T. J., & George, I. M. 1994, ApJ, 435, 106
Nowak, M. A., & Vaughan, B. A. 1996, MNRAS, 280, 227
Papadakis, I. E., & Lawrence, A. 1995, MNRAS, 272, 161
Pietrini, P., & Krolik, J. H. 1995, ApJ, 447, 526
Pounds, K. A., & Brandt, W. N. 1996, in X-Ray Imaging and Spectroscopy of Cosmic Hot Plasmas (Tokyo: University Academy Press), in press
Pounds, K. A., Nandra, K., Stewart, G. C., George, I. M., & Fabian, A. C. 1990, Nature, 344, 132
Pounds, K. A., Stanger, V. J., Turner, T. J., King, A. R., & Czerny, N. 1986, MNRAS, 224, 443
Poutanen, J., Sikora, M., Begelman, M. C., & Magdziarz, P. 1996, ApJ, 465, 107
Poutanen, J., & Svensson, R. 1996, ApJ, 470, 249
Ptak, A., Yaqoob, T., Serlemitsos, P. J., Mushotzky, R., & Otani, C. 1995, ApJ, 436, L31
Saxton, R. D., Turner, M. J. L., Williams, O. R., Stewart, G. C., Ohashi, T., & Kii, T. 1993, MNRAS, 262, 63
Shakura, N. I., & Sunyaev, R. A. 1973, A&A, 24, 337
Shapiro, S. L., Lightman, A. P., & Eardley, D. M. 1976, ApJ, 204, 187
Stern, B. E., Poutanen, J., Svensson, R., Sikora, M., & Begelman, M. C. 1995, ApJ, 449, L13
Sunyaev, R. A., & Titarchuk, L. G. 1980, A&A, 86, 121
Svensson, R. 1996, A&A, 55, in press
Tagliaferri, G., Bao, G., Israel, G. L., Stella, L., & Treves, A. 1996, ApJ, 465, 181
Titarchuk, L. G., & Mastichiadis, A. 1994, ApJ, 433, L33
Turner, T. J., George, I. M., & Mushotzky, R. F. 1993, ApJ, 412, 72
Turner, T. J., & Pounds, K. A. 1989, MNRAS, 240, 833
Ulrich-Demoulin, M.-H., & Molendi, S. 1996a, ApJ, 457, 77
———. 1996b, in MPE Report 263, Röntgenstrahlung from the Universe, ed. H. U. Zimmermann, J. E. Trümper, & H. Yorke (Berlin: Garching), 519
Walter, R., & Fink, H. H. 1993, A&A, 274, 105
Wilkes, B. J., & Elvis, M. 1987, ApJ, 323, 243
Zdziarski, A. A., Johnson, W. N., Done, C., Smith, D., & McNaron-Brown, K. 1995, ApJ, 438, L63
Zdziarski, A. A., Lightman, A. P., & Maciolek-Niedzwiecki, A. 1993, ApJ, 414, L93
Zdziarski, A. A., et al. 1994, MNRAS, 269, L55
Zdziarski, A. A., & Magdziarz, P. 1996, MNRAS, 279, L21